Deep Learning-Based Dynamic Spectrum Access for Coexistence of Aeronautical Communication Systems

David Kopyto[1], Sebastian Lindner[2], Leonard Schulz[1], Daniel Stolpmann[2], Gerhard Bauch[1], Andreas Timm-Giel[2]
Hamburg University of Technology, Institute of Communications[1], Institute of Communication Networks[2]
{david.kopyto, sebastian.lindner, leonard.schulz, daniel.stolpmann, bauch, timm-giel}@tuhh.de

***Abstract*—The historic assignments of frequency spectrum to communication systems has all but exhausted this resource. In consequence, novel systems such as *L*-band Digital Aeronautical Communications System Air-Air need to coexist with legacy systems, and must show not to cause excessive interference. The Distance Measuring Equipment (DME), the most critical legacy system in this case, expectedly allows the opportunistic use of a substantial number of idle communication resources, as our statistical model of the system reveals. We propose a Recurrent Neural Network to predict DME patterns reliably. Our architecture is based on a combination of Long Short-Term Memory (LSTM) and dense layers and was found with the help of hyperparameter optimization techniques. The predictor is trained and evaluated on a synthetic data set using realistic DME parameters. Furthermore, we introduce a baseline algorithm for comparison, which makes perfect predictions on a simplified periodic data set but breaks down for realistic scenarios. We argue that our Deep Learning approach can be used in realistic scenarios to detect idle resources given a strict constraint on correctly predicted busy resources.**

***Index Terms*—cognitive radio, coexistence, aeronautical communications, dynamic spectrum access**

I. Introduction

Frequency spectrum is a finite resource, and the historic allocations of bands to communication systems have nearly exhausted those that are suitable for radio communication. However, the Federal Communications Commission (FCC) has found that legacy systems rarely utilize licensed bands more than 38 % of the time [1]. It follows, that new communication systems must coexist with legacy systems increasingly often.

One such new communication system is the *L*-band Digital Aeronautical Communications System (LDACS), whose Air-Ground (A/G) component is currently being standardized by International Civil Aviation Organization (ICAO), and whose Air-Air (A/A) component is in the research phase. LDACS A/A will be allocated a frequency range in the aeronautical *L*-band, where several legacy communication systems operate – the most prominent one has been found to be Distance Measuring Equipment (DME) [2]–[5]. The DME system theoretically occupies nearly the entire frequency range of LDACS A/A, but practically a substantial amount of communication resources is left idle, as illustrated in Fig. 1. This paper studies the channel access behavior of the DME system. A Cognitive Radio (CR) approach is evaluated, in order to support LDACS A/A as a secondary user system within the primary user DME band. We develop a Deep Learning-based prediction method and compare it to a conventional baseline algorithm. This baseline algorithm works optimally on simplified channel access patterns, but breaks down for more realistic, irregular channel access patterns. For this reason we show how a Recurrent Neural Network (RNN) can find an internal representation of these pattern, even when they are highly irregular. Our results demonstrate that our proposed RNN architecture produces superior inference compared to the baseline algorithm in realistic scenarios.

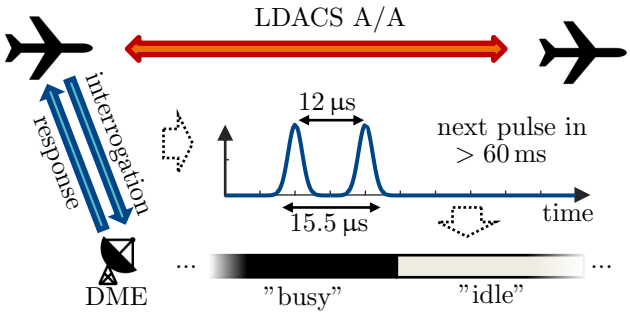

Figure 1: Exemplary depiction of two LDACS A/A users coexisting with a DME ground station. DME interrogator and response channel operate on different frequency bands. A DME pulse pair with a spacing of 12 µs is shown, resulting in a "busy" time slot for that duration. DME request pulses are scattered very sparsely over time, leaving substantial "opportunistic" resources for LDACS A/A.

In the following, the DME and LDACS A/A systems are discussed in Sec. II, and a statistical model of the expected number of opportunistically usable resources left over by DME is presented in Sec. III. The baseline and RNN approaches for DME pattern prediction are proposed in Sec. IV. We show simulation results of several coexistence scenarios between LDACS A/A and DME in Sec. V and conclude the document in Sec. VI.

II. The DME and LDACS A/A Systems

This section describes the possible coexistence between DME and LDACS A/A, which is illustrated in Fig. 2.

DME, described in [6], is an analog legacy system still used for localization of aircraft today. DME interrogators send short Gaussian pulse pairs on 1 MHz wide channels. After a delay of 50 µs, the corresponding ground station sends a response pulse on a different frequency at + or −63 MHz. Based on the propagation delay, the DME interrogator can then estimate its distance to the ground station, the coordinates of which are known. In order to establish a link, a DME interrogator enters *search mode*. However, 95 % of the time, the DME user will operate in *track mode*. According to its standard, a DME user is required to send no more than 16 pulse pairs per second (ppps) in track mode. In practice, DME users typically operate with as few as 5 ppps [7]. Hence, delays between pulses are 62.5-200 ms. Depending on local settings of the ground station, a DME user can operate in X-mode or in Y-mode. According to [7], most of the time X-mode is used, which will thus be focussed upon in this paper. In X-mode, the pulse pair spacing between the peaks is defined to be 12 µs, resulting in a total effective transmission time of 15.5 µs when considering rise and fall time of the pulses, as visualized in Fig. 1. In the DME response channels, additionally to response pulses, DME base stations send randomly distributed *squitter* pulses to maintain a minimum pulse repetition rate of 2700 ± 3.3 % ppps.

In contrast to DME, LDACS A/A is a new, digital, aeronautical communication standard, with a channel bandwidth of 500 kHz and time slot lengths of 6, 12 or 24 ms, depending on the channel quality. LDACS A/A will operate in the *L*-Band at 960–1215 MHz, and since DME is safety-critical, the interference that LDACS A/A causes upon DME must be minimized. Currently, even if only a single DME user operates in some interrogator channel, the frequencies for two full LDACS A/A channels are blocked to avoid interference. We instead propose to identify idle time slots in-between DME pulses, which could be opportunistically used by LDACS A/A. The squitter pulses in the response channels are transmitted at a high rate and cause constant interference with LDACS A/A. Hence, these channels bear no usable resources for LDACS A/A. Therefore, it is sufficient to discuss single-channel prediction on DME interrogator channels. In the following, we quantify the expected number of resources left for LDACS A/A in those channels.

III. Expectedly Available Resources

With the channel access characteristics of DME in-hand, we derive the lower bound of the expected number of time slots that will be available for opportunistic use for LDACS A/A. Consider the spectral view that one LDACS A/A user has of one DME request channel. Let l be the current LDACS A/A time slot length, and let n be the number of DME users currently operating on this channel and assume their request periodicity is maximum at $\tau = 62.5$ ms. After the first user's request transmission, all remaining

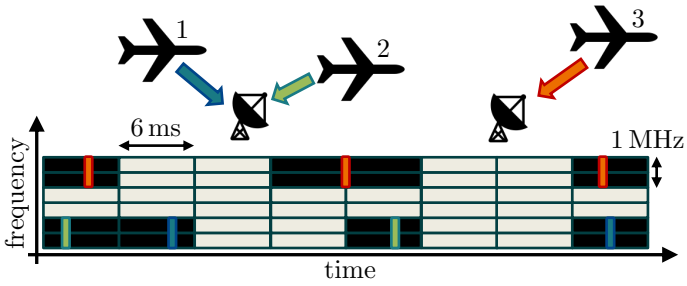

Figure 2: Exemplary local scenario of two DME ground stations with two and one connected airborne users, respectively. Users 1 (blue) and 2 (green) share one frequency band, which results in more occupied LDACS A/A slots than in the band where only user 3 (orange) operates. Note, that for illustration purposes, we depict a higher DME pulse periodicity than is used in practice. Response channels are not shown as their frequency bands are fully occupied by squitter pulses and not usable for LDACS A/A.

$n-1$ users must transmit their request within τ. As the DME transmission time is significantly shorter than that of LDACS A/A, the question of interest can be viewed as an instance of the well-known urn model. In-between the first and second DME user's transmissions, $m = \lfloor \frac{\tau}{l} \rfloor$ LDACS slots are idle from this user's transmissions – picture these as urns. Each remaining $n-1$ DME user randomly accesses the channel during one of these slots – places a ball in one of the urns. Alternatively, with a comparatively small probability, it transmits during the same LDACS slots used for the first user's transmissions. This is visualized in Fig 3. Fix the i^{th} urn, then we are

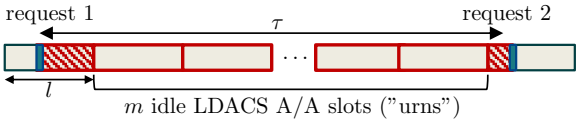

Figure 3: One DME user transmits two requests. The remaining $n-1$ users must place their transmissions in-between these two transmissions.

interested in the probability that it remains empty after all $n-1$ balls have been placed. Let X_i be a random variable that models whether the i^{th} urn remains empty. Each ball placement is a Bernoulli trial that puts the ball in the urn with probability p. There exists a probability q that the ball goes into the same urns as the first user's requests', so p is:

$$q = \frac{\frac{\tau}{l} - \lfloor \frac{\tau}{l} \rfloor}{\frac{\tau}{l}} \Rightarrow p = \frac{1-q}{m} \tag{1}$$

Let $Y_{n,m}$ be a random variable that models the number of empty urns after n ball placements into m urns, then as each urn remains empty according to a Binomial distribu-

tion, the expected number of empty urns is:

$$P(X_i = 1) = \cancel{\binom{m}{0}}^{1} \cancel{p^0}^{1} (1-p)^{n-1} = \left(\frac{m-1+q}{m}\right)^{n-1}$$
$$\Rightarrow \mathbf{E}[Y_{n,m}] = \sum_{i=1}^{m} 1 \cdot P(X_i = 1) = m \cdot \left(\frac{m-1+q}{m}\right)^{n-1} \tag{2}$$

Fig. 4 compares this model with simulations for the three time slot durations over an increasing number of DME users. It shows a perfect match between model and simulation, and highlights that the expected number of opportunistically usable resources increases drastically for shorter LDACS A/A time slot durations and fewer active DME users. For $l \in \{6, 12\,\text{ms}\}$, realistic numbers of DME users leave a substantial amount of idle time slots for LDACS to use, and these numbers increase further if DME users select less frequent request periodicities.

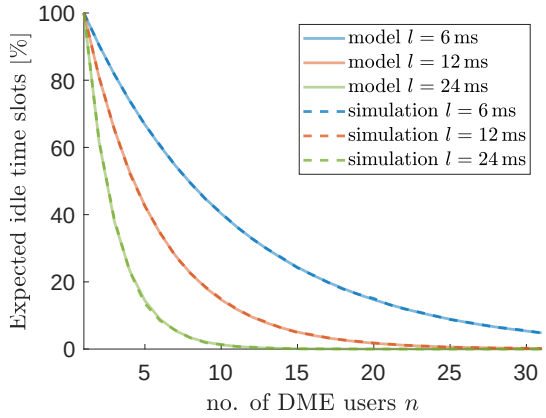

Figure 4: Validation of the expectation value for different time slot durations and numbers of DME users through a comparison with simulation.

IV. Prediction Methods for DME Patterns

This section first generates a data set, and then describes our prediction algorithm proposals that will be evaluated on the data set.

A. Synthetic Data Set Generation

We assume a stationary scenario, where all $\mathcal{U} = \{u_1, \ldots, u_n\}$ users are operating in track mode. Each user is parameterized by a uniformly random period $\tau_i \in [62.5\,\text{ms}, 200\,\text{ms}]$, and a uniformly random start offset $o_i \in [0\,\text{ms}, 200\,\text{ms}]$. The second describes the time of the first request transmission, and the first the time in-between further requests. Each transmission lasts 15.5 µs. We mark an LDACS A/A slot t as "busy" if at least one DME request overlaps with it, yielding

$$O_{\mathcal{U}}(t) = \begin{cases} 0, & \text{if no DME user has transmitted} \\ 1, & \text{else} \end{cases} \tag{3}$$

Formally, our goal is to predict the observation $O_{\mathcal{U}}(k)$ at a fixed time k, given the history $H_{k-1} = \{O_{\mathcal{U}}(1), O_{\mathcal{U}}(2), , \ldots, O_{\mathcal{U}}(k-1)\}$ of all previous observations. It should be emphasized, that the parameters of the users are not known. Further, note that DME periods τ and LDACS A/A time slot lengths l do not necessarily align, i.e. $\frac{\tau}{l} \in \mathbb{N}$ does not always hold. Therefore, $O_{\mathcal{U}}$ is not generally periodic – even for a single user – which complicates predictions.

B. Baseline Algorithm

For the simplified case, where the DME periodicity aligns with the LDACS slot length, we can construct an optimal algorithm to solve the prediction problem. Here, we leverage our expert knowledge in that we only need to find the *parameterization* $\mathcal{U}$ to perfectly predict the pattern $O_{\mathcal{U}}$. If $\frac{\tau}{l}$ is an integer, we can also assume o to be an integer, therefore only a finite number of possible parameterizations $\mathcal{U}$ exist. Alg. 1 first generates the set of all possible DME user parameters $\hat{\mathcal{U}}$ and then reduces it to the actual $\mathcal{U}$ by using one argument: If an LDACS A/A slot is "idle", but the parameters of a DME user would have led to the slot being "busy", then these parameters cannot be a part of $\mathcal{U}$.

Algorithm 1 Baseline algorithm for pattern prediction

Require: History H_{k-1}
  for $i = 1, \ldots, k-1$ **do**
    if $i < \tau_{\max}$ **then**
      for $\tau \in \{\tau_{\min}, \ldots, \tau_{\max}\}$, $o \in \{o_{\min}, \ldots, o_{\max}\}$ **do**
        $\hat{\mathcal{U}} \leftarrow \hat{\mathcal{U}} \cup (\tau, o)$
    if $H_{k-1}(i) = 0$ **then**
      for $u \in \hat{\mathcal{U}}$ **do**
        if $O_u(i) = 1$ **then** $\hat{\mathcal{U}} \leftarrow \hat{\mathcal{U}} \setminus u$
  return $\hat{\mathcal{U}}$

The baseline algorithm does not work when $\frac{\tau}{l} \notin \mathbb{N}$, and requires knowledge of the data set. We address both of these issues in the following section where we train an RNN which can deal with highly irregular patterns by extracting expert knowledge about the data set automatically.

C. Deep Learning Algorithm

We propose an RNN for pattern prediction that extends our previous work in [8] and is also related to [9], where DNA patterns were predicted using an architecture similar to ours.

1) Architecture: We propose the RNN displayed in Fig. 5, which consists of a combination of LSTM and dense layers. While we found the exact architecture with the help of hyperparameter search using Hyperopt [10], an intuitive explanation of the network is as follows: The last L observations are provided one-by-one as an input sequence to the first LSTM layer, where temporal

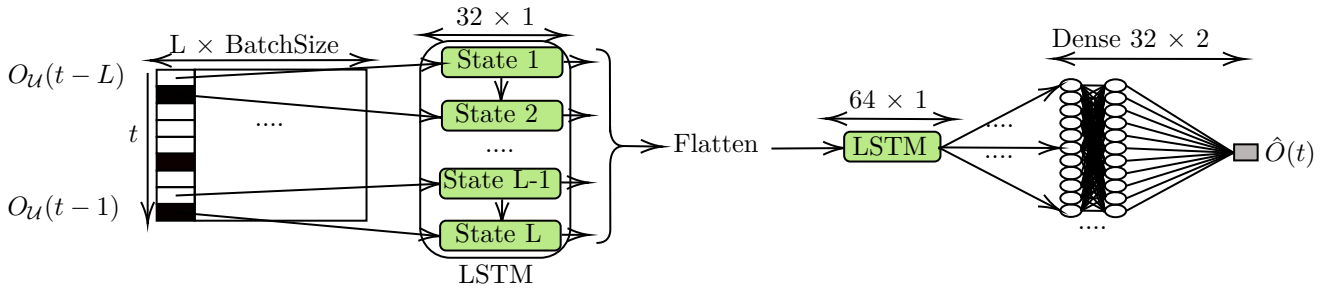

Figure 5: Architecture for hyperparameter search and training. A batch of training sequences is input and fed through an Long Short-Term Memory (LSTM) layer, whose hidden states are flattened and the resulting vector is fed to a second LSTM layer, which learns temporal relations over multiple input sequences by not resetting the hidden states. The LSTM result is fed to dense layers and mapped to a single time step prediction $\hat{O}(t)$, that is a soft estimation of $O_{\mathcal{U}}(t)$.

relations between them are inferred. The hidden states over time are flattened, passed to another LSTM layer and reset afterwards. This LSTM layer again computes temporal relations, but now over multiple input sequences by not resetting the hidden states. The outputs are given to a stack of two dense layers, which decode the latent representation into a soft output for the predicted state of the next time slot.

2) Training: In order to have our model implicitly learn about the underlying structure of DME channel access behavior, we trained the RNN on several different parameterizations of $\mathcal{U}$ and resulting patterns. This is fundamentally different from our previous work in [8], where training was done purely online on a single pattern. One training batch consisted of 128 different patterns, each resulting from a randomly sampled number of users $n = 1, ..., 15$, where each user in the pattern has a different parameterization $\mathcal{U}$. The input length for each pattern was set to a "sliding window" of length $L = 128$. For 2500 steps per epoch, the window was shifted by one time step and fed into the network. We trained for a total of 25 epochs and optimized the weights using the Adam optimizer with the Binary Cross Entropy loss.

3) Evaluation: Evaluation is done on a batch of 32 patterns in the same manner as the training process. To test whether the RNN learned underlying structure of the data set, different patterns were used for evaluation than for training. The accuracy, which is commonly used in Deep Learning applications, is not a suitable metric for the binary detection problem at hand for two reasons. Firstly, for a low number of DME users, the pattern is very sparse, and a predictor outputting only "idle" would have a good accuracy, but not solve our problem. Secondly, the application requires that the predictor avoids interference with DME very reliably. Predicting a *busy* time slot as *busy* ("true positive") should therefore happen with a high rate. On the other hand, predicting an *idle* time slot as *busy* ("false positive") corresponds to missing a slot that would have been usable for LDACS A/A and is less problematic.

Consequently, as an alternative to accuracy, we consider

$O_{\mathcal{U}}(t)$	1	0	0	1	0	1	1	0	0
$\hat{O}(t)$	0.5	0.4	0.1	0.9	0.5	0.3	0.9	0.1	0.1
Result	1	1	0	1	1	1	1	0	0

Figure 6: Down-sized example of a prediction result while demanding that TPR = 1. To get all busy channels correctly classified, the threshold on $\hat{O}(t)$ has to be at least 0.3. The resulting FPR is then FPR $= \frac{2}{5} = 40\%$.

the true positive rate (TPR)

$$\text{TPR} = \frac{\#\text{ busy slots, where } \textit{prediction} = \text{busy}}{\#\text{ total busy slots}}, \quad (4)$$

and the false positive rate (FPR)

$$\text{FPR} = \frac{\#\text{ idle slots, where } \textit{prediction} = \text{busy}}{\#\text{ total idle slots}}, \quad (5)$$

instead. Plotting the FPR over the TPR results in the Receiver Operating Characteristic (ROC), a common performance metric in CR [11]. To mitigate interference of DME and LDACS A/A reliably, our predictor should satisfy TPR ≈ 1. For clarification, we provide an example output of our predictor in Fig. 6. One can improve the TPR by employing a threshold, at the cost of a worse FPR. This tradeoff can further be quantified by measuring the Area Under Curve (AUC) of the ROC (larger is better). We used the AUC as the metric to maximize during hyperparameter tuning (see Sec. IV-C1).

V. Results

The ROC curve results for our predictors are shown in Fig. 7. For each number of users $n = 1, \ldots, 15$ the mean ROC curves for 32 patterns each are plotted together with the 95% confidence intervals. We ignore the network warm-up time by starting evaluation after an initial 2500 time slots. The AUCs expectedly decrease with the number of users, as pattern complexity increases with the number of users, making it harder for the RNN to predict the next time slot. The baseline algorithm is given for comparison,

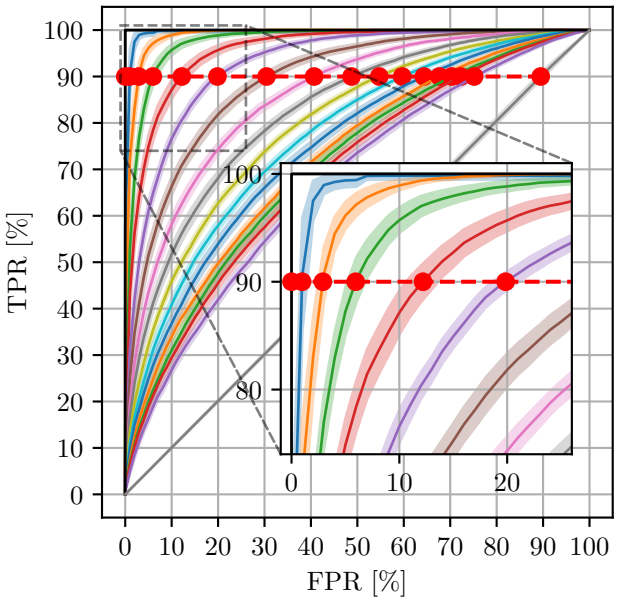

Figure 7: *In colors*: mean ROC curves and 95 % confidence intervals for different numbers of users $n = 1, \ldots, 15$ from left to right with decreasing AUC for increasing n. The RNN was trained on patterns with $\frac{\tau}{l} \notin \mathbb{N}$. For comparison, the ROC curves for the baseline algorithm are shown. *Black*: For $\frac{\tau}{l} \in \mathbb{N}$ the algorithm performs perfect prediction (AUC=1). *Grey*: For $\frac{\tau}{l} \notin \mathbb{N}$, the baseline performs random guessing (AUC=0.5).

which perfectly predicts patterns with $\frac{\tau}{l} \in \mathbb{N}$. Since it has been designed to reliably avoid interference, it also shows a perfect ROC curve. In contrast, for $\frac{\tau}{l} \notin \mathbb{N}$, the algorithm breaks down and yields no useful results.

The ROC curves in Fig. 7 can now be used to assess the number of predictable idle time slots in a dedicated frequency band of LDACS A/A, when a constraint on the minimum amount of correctly classified busy slots (TPR) needs to be met. Analogously to the toy example from Fig. 6, one can apply a threshold on the ROC curve in Fig. 7. For example when setting a requirement of TPR $> 90\,\%$, for $n = 2$, only around $3\,\%$ of idle slots would be lost. For $n = 5$ users, our algorithm is able to detect around $80\,\%$ of idle slots when a constraint of detecting $90\,\%$ of busy slots needs to be met. Joining this with our statistical model from Sec. III, this means that more than $55\,\%$ of resources in a DME interrogator channel with 5 users can be used for LDACS A/A. For up to $n = 15$ users, resources can still be detected, where the total number of detectable resources decreases with n, due to lower AUC, and lower total amount of expected usable resources as explained in Sec. III. In summary, our Deep Learning-based approach shows promising results for the numbers of users that were considered, motivating its application for coexistence between LDACS A/A and DME.

VI. Conclusion

In this paper, we have investigated a form of coexistence between LDACS A/A and DME through dynamic spectrum access. First, a statistical model has shown that under realistic system loads, a sufficient amount of radio resource is left idle by DME. Both a baseline and a Deep Learning-based algorithm were proposed to predict future DME channel accesses. As the baseline algorithm fails under realistic assumptions, the application of a RNN is motivated. Results show that the RNN is capable of correctly identifying a high number of idle resources. Future work should consider user mobility and the corresponding changes in DME channel access patterns, and should investigate whether the algorithm can adapt quickly enough.

References

[1] H.-H. Chang, H. Song, Y. Yi, J. Zhang, H. He, and L. Liu, "Distributive Dynamic Spectrum Access through Deep Reinforcement Learning: A Reservoir Computing Based Approach," *IEEE Internet of Things Journal*, vol. 6, no. 2, pp. 1938–1948, Apr. 2019.

[2] M. Mostafa, M. A. Bellido-Manganell, and T. Gräupl, "Feasibility of Cell Planning for the L-Band Digital Aeronautical Communications System Under the Constraint of Secondary Spectrum Usage," *IEEE Transactions on Vehicular Technology*, vol. 67, no. 10, pp. 9721–9733, Oct. 2018.

[3] U. Epple and M. Schnell, "Overview of Interference Situation and Mitigation Techniques for LDACS," in *2011 IEEE/AIAA 30th Digital Avionics Systems Conference*, 2011.

[4] U. Epple, F. Hoffmann, and M. Schnell, "Modeling DME interference impact on LDACS1," in *2012 Integrated Communications, Navigation and Surveillance Conference*, Herndon, VA, USA, Apr. 2012, G7-1-G7–13.

[5] M. A. Bellido-Manganell and M. Schnell, "Feasibility of the Frequency Planning for LDACS Air-to-Air Communications in the L-band," in *2021 Integrated Communications, Navigation and Surveillance Conference (ICNS)*, Apr. 2021.

[6] European Organization for Civil Aviation Equipment (EUROCAE), *Minimum Operational Performance Requirements for Distance Measuring Equipment Interrogator (DME/N and DME/P) Operating Within the Radio Frequency Range 960 to 1215 MHz*, Jan. 1987.

[7] S. C. Lo and P. Enge, "Assessing the Capability of Distance Measuring Equipment (DME) to Support Future Air Traffic Capacity: Study of DME Capacity to Support Future Air Traffic," *Navigation*, vol. 59, no. 4, pp. 249–261, Dec. 2012.

[8] S. Lindner, L. Fisser, and A. Timm-Giel, "Coexistence of Shared-Spectrum Radio Systems through Medium Access Pattern Learning using Artificial Neural Networks," in *2020 32nd International Teletraffic Congress (ITC 32)*, Sep. 2020, pp. 165–173.

[9] X. Gao, J. Zhang, and Z. Wei, "Deep learning for sequence pattern recognition," in *2018 IEEE 15th International Conference on Networking, Sensing and Control (ICNSC)*, Mar. 2018, pp. 1–6.

[10] J. Bergstra, D. Yamins, and D. D. Cox, "Making a science of model search: Hyperparameter optimization in hundreds of dimensions for vision architectures," in *Proceedings of the 30th International Conference on International Conference on Machine Learning*, ser. ICML'13, vol. 28, Atlanta, GA, USA, Jun. 2013, pp. I-115–I-123.

[11] S. Atapattu, C. Tellambura, and H. Jiang, "Energy Detection Based Cooperative Spectrum Sensing in Cognitive Radio Networks," *IEEE Transactions on Wireless Communications*, vol. 10, no. 4, pp. 1232–1241, Apr. 2011.